PHYSICAL REVIEW D VOLUME 35, NUMBER 1 1 JANUARY 1987

Nucleon-nucleon partial-wave analysis to 1100 MeV

Richard A. Arndt, John S. Hyslop III, and L. David Roper
Department of Physics, Virginia Polytechnic Institute and State University, Blacksburg, Virginia 24061
(Received 11 September 1986)

Comprehensive analyses of nucleon-nucleon elastic-scattering data below 1100 MeV laboratory kinetic energy are presented. The data base from which an energy-dependent solution and 22 single-energy solutions are obtained consists of 7223 *pp* and 5474 *np* data. A resonancelike structure is found to occur in the $^1D_2$, $^3F_3$, $^3P_2$-$^3F_2$, and $^3F_4$-$^3H_4$ partial waves; this behavior is associated with poles in the complex energy plane. The pole positions and residues are obtained by analytic continuation of the "production" piece of the T matrix obtained in the energy-dependent solution. The new phases differ somewhat from previously published VPI&SU solutions, especially in $I=0$ waves above 500 MeV, where *np* data are very sparse. The partial waves are, however, based upon a significantly larger data base and reflect correspondingly smaller errors. The full data base and solution files can be obtained through a computer scattering analysis interactive dial-in (SAID) system at VPI&SU, which also exists at many institutions around the world and which can be transferred to any site with a suitable computer system. The SAID system can be used to modify solutions, plan experiments, and obtain any of the multitude of predictions which derive from partial-wave analyses of the world data base.

I. INTRODUCTION

Our continuing analysis of *NN* scattering data has been constantly available on VPI&SU and many other computers around the world for several years. Because of recent additions of many very precise *NN* scattering data to the world data base, we present here a summary of the status of the analysis in the middle of 1986.

Section II contains a description of the elastic nucleon-nucleon scattering data base used for this analysis. Section III is a description of the energy-dependent parametrization used. In Sec. IV we report results for the 23 analyses of this paper. In Sec. V an interpretation is presented for the $^1D_2$, $^3F_3$, $^3P_2$-$^3F_2$, and $^3F_4$-$^3H_4$ resonancelike structures; complex-plane pole positions and residues are given. Section VI is a summary of our results.

II. NUCLEON-NUCLEON ELASTIC-SCATTERING DATA BASE

The last *NN* scattering analyses published by the VPI&SU group[1] employed 5207 *pp* data below 1.2 GeV and 5283 *np* data below 1.1 GeV. The present data base contains 7223 *pp* data and 5474 *np* data over the same energy range. Most of the new data are above 500 MeV and have produced substantial improvements in the higher-energy phases for both $I=1$ and 0. Figure 1 is a kinematic distribution plot of data added since 1982. The numbers on Fig. 1 do not quite add up to the difference between our 1982 and 1986 totals because of the dynamic character of the data base; some data are included as "preliminary" and are subsequently replaced by published values.

above 500 MeV in both numbers and data types. Since most of the new data are from high-intensity accelerators, the statistical quality gives them added weight against the

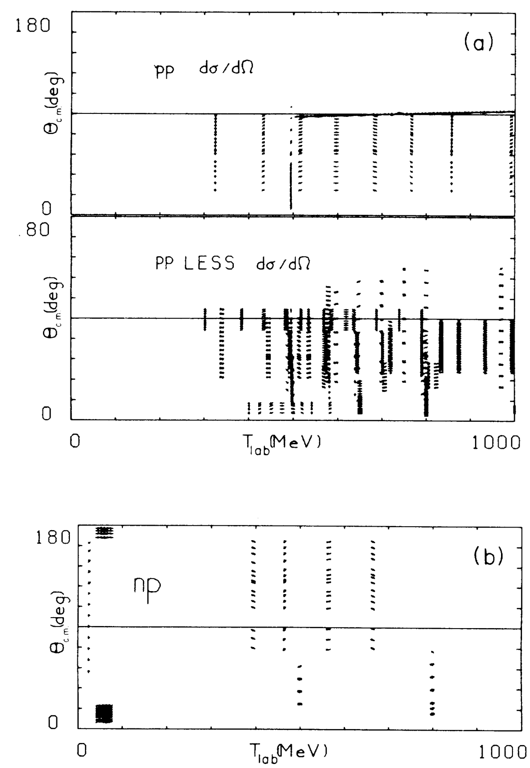

FIG. 1. Distribution plots of recent *pp* (a), and *np* (b) data. *pp* data are [observable (number of data)]: $d\sigma/d\omega$ (306), P (434), D (61), D_t (24), A_{yy} (268), A_{xx} (97), A_{zz} (395), A_{zx} (115), R (64), R' (40), A (64), A' (58), σ_1 (37), and σ_t (22). *np* data are P (76), D (7), A_{yy} (60), R (13), R' (13), A (10), A' (10).

older data base. The improvement in np observables is much less impressive but, if the nearly 4000 (mostly charge exchange) cross sections in the np data base are ignored, a significant improvement is revealed. As in the case of the pp data base, most of the new data are of higher quality and at higher energies than the older data.

An important change in the np data base has been the addition of very precise LAMPF total cross sections[2] from 40 to 770 MeV. As shown in Fig. 2, this causes the predicted values of cross section between 200 and 500 MeV to change by about 5% from the previous solution.

Data added in recent years have exacerbated the dramatic imbalance between pp data and np data, the latter of which is the only handle on the $I=0$ scattering amplitudes. This should be partially remedied in the next few years as planned np experiments are run, but the imbalance will persist into the foreseeable future.

III. PARAMETRIZATION OF THE ENERGY-DEPENDENT SOLUTION SM86

The representation presently being used for energy-dependent solution SM86 differs from that used previously in that the S matrix is decomposed into an "exchange" piece S_x and a "production" piece S_p. The full S matrix is then given by

$$S=S_x{}^{1/2}S_pS_x{}^{1/2}=1+2iT ,$$

where (1)

$$T=T_x+S_x{}^{1/2}T_pS_x{}^{1/2} .$$

The "exchange" piece S_x is parametrized through a K matrix K_x which is expanded as a sum of one-pion exchange plus a sum over expansion bases containing appropriate left-hand cuts.[3] S_x is a smoothly varying elastic function. The production piece S_p is expanded by a Chew-Mandelstam coupled-channel K-matrix form as described in our recent πN analysis.[4] S_p contains the $N\Delta$ branch cut and presumably implicitly contains the dibaryon poles responsible for resonancelike structure in a number of partial waves. The analytic construction of S_p allows a mapping of T_p in the complex energy plane and thereby a determination of the positions and residues of important poles.

For spin-uncoupled states $({}^1D_2, {}^3F_3, \ldots)$ the procedure is simple:

$$T_p=\rho^{1/2}K_p(1-CK_p)^{-1}\rho^{1/2} , \tag{2}$$

where C is the 2×2 diagonal Chew-Mandelstam matrix

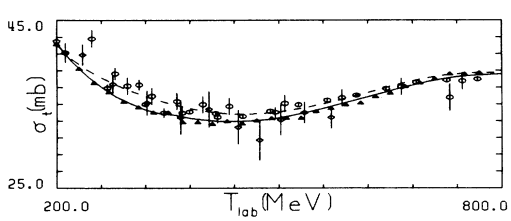

FIG. 2. np total cross sections for 200–800 MeV. Solid curve is solution SM86; dashed curve is solution SP82.

and K_p is a 2×2 real symmetric matrix which couples the elastic (NN) channel to the appropriate $N\Delta$ channel. K_p can be written

$$K_p=\begin{bmatrix} K_e & K_0 \\ K_0 & K_i \end{bmatrix} . \tag{3}$$

Its elements are then expanded as polynomials in the energy $W_{\rm c.m.}$, and the "production" T matrix T_p is as given in Eq. (2). In practice, we use $K_e=0$ and only one or two terms are necessary for K_0 and K_i. T_p is then combined with the "exchange" piece

$$T_x=\frac{K_x}{1-iK_x} \tag{4}$$

to form the full T matrix

$$T=\frac{K_x}{1-ik_x}+\frac{1+iK_x}{1-iK_x}T_p$$

$$=\exp(i\delta_x)\sin\delta_x+\exp(2i\delta_x)T_p , \tag{5}$$

where

$$\delta_x=\arctan K_x .$$

The spin-coupled states $({}^3P_2\text{-}{}^3F_2, {}^3S_1\text{-}{}^3D_1, \ldots)$ present more of a challenge. T_p must be obtained as the 2×2 elastic piece of a 3×3 matrix which couples the two elastic channels to the appropriate $N\Delta$ channel. The underlying K matrix K_p is now 3×3 and real symmetric and is representable as

$$K_p=\begin{bmatrix} K_e^- & K_e^0 & K_0^- \\ K_e^0 & K_e^+ & K_0^+ \\ K_0^- & K_0^+ & K_i \end{bmatrix} . \tag{6}$$

Each element is expandable in $W_{\rm c.m.}$, although in practice we set $K_e^-=K_e^0=K_e^+=0$ and only one or two terms are necessary for K_0^-, K_0^+, and K_i.

T_x (or S_x) can be obtained from a 2×2 K_x by

$$S_x=1+2iT_x=(1+iK_x)(1-iK_x)^{-1} ,$$

where (7)

$$K_x=\begin{bmatrix} K_x^- & K_x^0 \\ K_x^0 & K_x^+ \end{bmatrix} .$$

Since K_x is real symmetric it can be diagonalized with a rotation whose columns are the normalized eigenvectors of K_x. That is, K_x can be written

$$K_x=R\begin{bmatrix} \Lambda_- & 0 \\ 0 & \Lambda_+ \end{bmatrix}R^T , \tag{8}$$

where

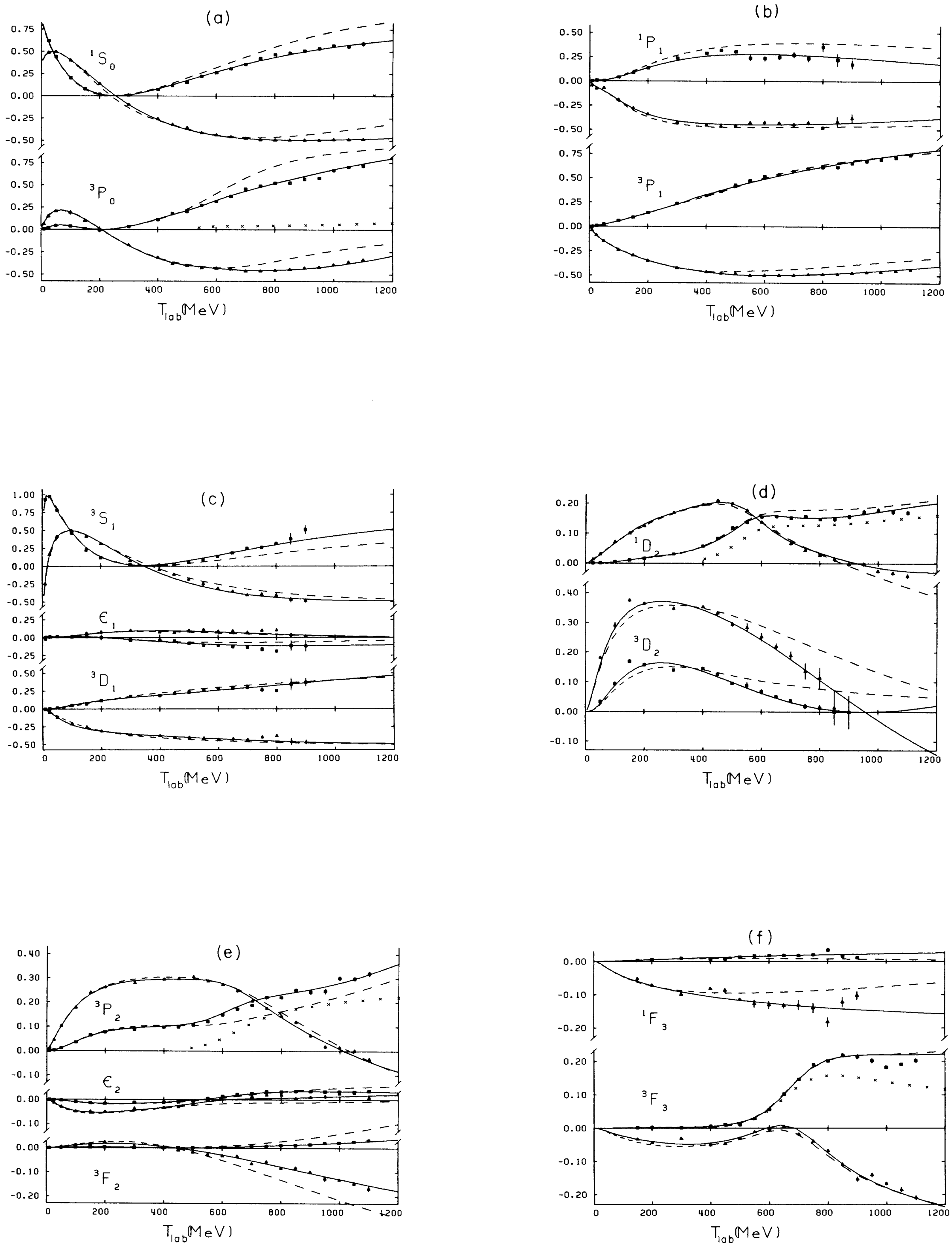

FIG. 3. Partial-wave amplitudes for 0–1200 MeV. Solid curves are solution SM86; dashed curves are solution SP82. The symbols are ▲ = ReT, ■ = ImT, and $X = \mathrm{Im}T - T^2 - T_{sf}^2$, where T_{sf} = spin-flip amplitude.

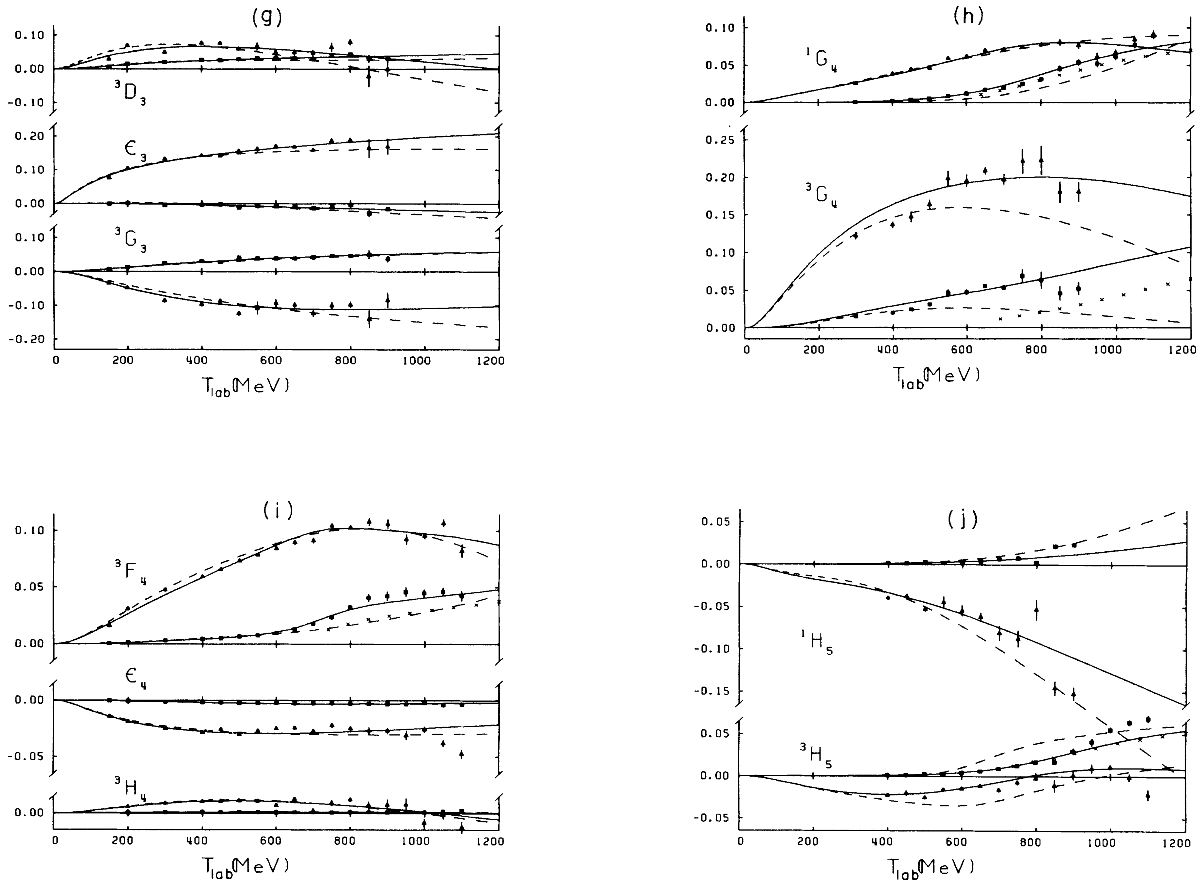

FIG. 3. (*Continued*).

$$R=\begin{bmatrix}\cos\phi & \sin\phi\\ -\sin\phi & \cos\phi\end{bmatrix}$$

in terms of a rotation angle ϕ. Λ_- and Λ_+ are the eigenvalues of K_x and R is constructed so that

$$R^TK_xR=\begin{bmatrix}\Lambda_- & 0\\ 0 & \Lambda_+\end{bmatrix}. \tag{9}$$

S_x and $S_x{}^{1/2}$ can now be written

$$S_x=R\begin{bmatrix}\dfrac{1+i\Lambda_-}{1-i\Lambda_-} & 0\\ 0 & \dfrac{1+i\Lambda_+}{1-i\Lambda_+}\end{bmatrix}R^T$$

and (10)

$$S_x{}^{1/2}=R\begin{bmatrix}\dfrac{1+i\Lambda_-/2}{1-i\Lambda_-/2} & 0\\ 0 & \dfrac{1+i\Lambda_+/2}{1-i\Lambda_+/2}\end{bmatrix}R^T.$$

Defining

$$t_\pm\equiv\frac{\Lambda_\pm}{1-i\Lambda_\pm}$$

and

$$S_\pm\equiv\frac{1+i\Lambda_\pm/2}{1-i\Lambda_\pm/2},$$

the full T matrix can be calculated as

$$T=R\left[\begin{bmatrix}t_- & 0\\ 0 & t_+\end{bmatrix}+\begin{bmatrix}S_- & 0\\ 0 & S_+\end{bmatrix}R^TT_pR\begin{bmatrix}S_- & 0\\ 0 & S_+\end{bmatrix}\right]R^T.$$

IV. SUMMARY OF SOLUTIONS

Single-energy solutions were obtained at 22 energies from 10 to 1100 MeV by binning the data in a range about the central energy and then fixing the energy derivatives of the partial-wave parameters from the energy-dependent solution SM86. An appropriate number of phase parameters were then searched to obtain a minimal χ^2 fit to the selected data. A summary of these fits is given in Table I. The quantity identified as χ^2(SM86) is the value of χ^2 for the selected data as obtained from solution SM86. We developed the single-

TABLE I. Summary of nucleon-nucleon solutions to 1100 MeV. χ^2(SM86) is the χ^2 value for the selected data as obtained from solution SM86.

Solution	Range (MeV)	Parameters	pp data[χ^2(SM86)]	np data[χ^2(SM86)]
SM86	0–1100	115	7223/11900	5474/8871
C10	8–18	6	183/161[254]	102/84[112]
C25	15–35	9	65/42[56]	226/185[216]
C50	36–64	11	152/145[268]	283/312[361]
C100	85–110	11	112/79[105]	210/265[319]
C150	125–175	17	220/194[298]	253/318[385]
C200	179–225	17	81/82[113]	276/495[539]
C300	275–325	21	215/238[238]	473/625[814]
C400	375–425	25	342/362[441]	413/700[825]
C450	425–475	26	326/396[473]	338/447[536]
C500	425–525	29	695/890[1077]	378/483[648]
C550	520–580	29	671/810[891]	259/314[385]
C600	560–640	30	823/1086[1179]	487/586[675]
C650	610–690	31	636/725[769]	589/715[757]
C700	665–735	32	518/601[671]	349/386[446]
C750	705–795	36	575/812[962]	380/574[591]
C800	775–825	37	783/1434[1658]	332/566[692]
C850	810–890	37	359/493[602]	150/205[293]
C900	850–950	39	323/468[613]	230/329[412]
P950	920–980	24	299/497[646]	73/109[125]
P999	960–1040	24	591/926[1044]	176/408[453]
P105	1000–1100	24	405/720[890]	167/434[474]
P110	1050–1150	24	170/301[368]	152/370[617]

energy solutions concurrently with the energy-dependent solution to use the single-energy results as a guide in the parametrization of SM86. We were particularly sensitive to systematic, with energy, deviations between the single-energy phases and values obtained from solution SM86. We interpret the results displayed in Fig. 3 to indicate no missing structures and to show a decent consistency between the global and local solutions.

In Table II the phase parameters with errors are summarized for the twenty-two single-energy solutions; phase parameters (δ,ρ) are as defined in our previous paper.[1]

To indicate the extent of change induced by recent data additions, superimposed in Fig. 3 are the partial waves from our previously published solution SP82 (dashed curves).[1] The changes appear to be substantial in certain partial waves, especially $I=0$ waves above 500 MeV. Some of the changes are probably related to the changed parametrization for energy dependence; SM86 contains 73 variable $I=1$ phases and produces a better (by about 1500 χ^2) fit to the pp data base than does SP82 when its 77 $I=1$ parameters are adjusted for minimum χ^2 against the present data base. In Fig. 4 the solutions are compared at 800 MeV, where many data have been added, by plotting some pp and np observables.

The relative importance of different partial waves to elastic or inelastic scattering is best measured by the partial-wave total and reaction cross sections, as plotted in Fig. 5. The buildup in $I=1$ waves as $T_{\rm lab}$ increases from 400 MeV is due to the rapid increase in reaction cross sections. The $I=0$ cross section reveals very little inelasticity and a slowly declining total cross section.

V. DIBARYONS: POSITIONS AND RESIDUES

These analyses produce clear resonancelike structures in four partial waves, $^1D_2$, $^3F_3$, $^3P_2$-$^3F_2$, and $^3F_4$-$^3H_4$. In Fig. 6 are plotted the corresponding T matrices from 2000 to 2400 MeV (c.m.) and for imaginary energies between -200 and 0 MeV. Our analytic representation for T_p can then be used to extract the positions and residues of poles which are clearly related to the "observed structures" (i.e., structures which have an effect on the real axis). The values so obtained are summarized in Table III. The $^3P_2$-$^3F_2$ and $^3F_4$-$^3H_4$ poles also exist, respectively, in the spin mixing amplitudes ϵ_2 and ϵ_4; but, since the residue function $G=(W_p-W)T$ is factorizable at the pole, only the residue for diagonal states need be reported.

The four resonant amplitudes have tightly constrained observed energy structures, and it is our belief that it would be very difficult to fit these waves precisely with analytic forms containing a reasonable representation of the important $N\Delta$ branch cut without generating the poles.

The strong inelasticity of all three poles and their positions relative to the important $N\Delta$ branch point at $2160-i\,50$ MeV, suggests an interpretation of the poles as conventional particle states of the $N\Delta$ channel. The branch cut, which is clearly visible in Fig. 6, is extended to the right for the $N\Delta$ S wave, which couples to $^1D_2$, and to the left for the $N\Delta$ P waves, which couple to $^3F_3$ and $^3P_2$-$^3F_2$. The $^3F_4$-$^3H_4$ state couples to an $N\Delta$ F wave. The evidence for a $^3F_4$-$^3H_4$ pole is weaker than for the

TABLE II. Nucleon-nucleon phases from single-energy analyses.

State	δ or ϵ (deg)	δ_{pp}-δ_{np} (deg)	ρ
		10.00 MeV	
$^3P_0$	3.65±0.04	−0.27	
$^1P_1$	−2.71±1.11	−0.27	
$^3P_1$	−2.18±0.02	0.14	
$^3S_1$	104.70±0.74	0.02	
$^3D_1$	−0.75±0.03	−0.02	
$^3P_2$	0.70±0.01	−0.08	
		25.00 MeV	
$^1S_0$	51.83±0.22	−3.34	
$^3P_0$	8.57±0.14	−0.32	
$^1P_1$	−4.53±0.45	−0.37	
$^3P_1$	−5.08±0.07	0.20	
$^3S_1$	80.44±0.67	0.02	
ϵ_1	0.69±0.50	0.00	
$^3D_1$	−2.92±0.02	−0.05	
$^1D_2$	0.71±0.03	−0.01	
$^3P_2$	2.56±0.04	−0.17	
		50.00 MeV	
$^1S_0$	41.60±0.13	−2.64	
$^3P_0$	11.93±0.23	−0.29	
$^1P_1$	−4.11±0.57	−0.31	
$^3P_1$	−8.58±0.07	0.27	
$^3S_1$	61.81±0.32	0.06	
ϵ_1	0.92±0.85	−0.02	
$^3D_1$	−7.04±0.17	−0.08	
$^1D_2$	1.68±0.04	−0.05	
$^3D_2$	10.69±0.27	0.10	
$^3P_2$	5.92±0.05	−0.27	
ϵ_2	−1.67±0.05	0.01	
		100.00 MeV	
$^1S_0$	26.68±0.49	−2.09	
$^3P_0$	11.07±1.47	−0.14	
$^1P_1$	−11.38±1.15	−0.08	
$^3P_1$	−14.38±0.28	0.35	
$^3S_1$	42.67±0.60	0.23	
ϵ_1	1.15±0.93	−0.06	
$^3D_1$	−12.73±0.35	−0.09	
$^1D_2$	4.04±0.13	−0.14	
$^3D_2$	17.86±0.77	0.07	
$^3P_2$	10.49±0.18	−0.38	
ϵ_2	−2.86±0.12	0.05	
		150.00 MeV	
$^1S_0$	16.36±0.46	−1.70	
$^3P_0$	5.48±0.44	0.03	
$^1P_1$	−16.98±0.88	0.13	
$^3P_1$	−18.02±0.14	0.41	
$^3S_1$	28.10±0.46	0.41	
ϵ_1	3.54±0.51	−0.10	
$^3D_1$	−15.29±0.38	−0.11	
$^1D_2$	5.77±0.08	−0.23	
$^3D_2$	24.29±0.50	0.04	
$^3P_2$	14.45±0.10	−0.45	
ϵ_2	−2.92±0.06	0.07	
$^3F_2$	0.87±0.18	0.06	
$^1F_3$	−3.03±0.31	−0.02	

TABLE II. (*Continued*).

State	δ or ϵ (deg)	δ_{pp}-δ_{np} (deg)	ρ
		150.00 MeV	
$^3F_3$	-1.91 ± 0.14	-0.05	
$^3D_3$	1.73 ± 0.34	-0.26	
ϵ_3	4.39 ± 0.18	0.10	
$^3F_4$	0.94 ± 0.09	0.01	
		200.00 MeV	
$^1S_0$	7.94 ± 0.43	-1.36	
$^3P_0$	-0.49 ± 0.42	0.18	
$^1P_1$	-21.52 ± 0.65	0.30	
$^3P_1$	-22.11 ± 0.18	0.45	
$^3S_1$	19.78 ± 0.58	0.56	
ϵ_1	4.39 ± 0.34	-0.13	
$^3D_1$	-19.43 ± 0.53	-0.14	
$^1D_2$	7.20 ± 0.13	-0.30	
$^3D_2$	23.39 ± 0.47	0.03	
$^3P_2$	15.89 ± 0.14	-0.50	
ϵ_2	-3.00 ± 0.09	0.09	
$^3F_2$	1.38 ± 0.19	0.06	
$^1F_3$	-4.14 ± 0.25	0.00	
$^3F_3$	-2.52 ± 0.13	-0.05	
$^3D_3$	4.13 ± 0.33	-0.32	
ϵ_3	6.06 ± 0.14	0.11	
$^3F_4$	1.80 ± 0.10	0.01	
		300.00 MeV	
$^1S_0$	-5.62 ± 0.34	-0.85	
$^3P_0$	-10.07 ± 0.46	0.44	
$^1P_1$	-29.17 ± 0.76	0.53	
$^3P_1$	-29.25 ± 0.26	0.51	
$^3S_1$	4.39 ± 0.75	0.76	
ϵ_1	6.14 ± 0.34	-0.16	
$^3D_1$	-24.28 ± 0.53	-0.22	
$^1D_2$	9.92 ± 0.11	-0.41	1.54 ± 0.00
$^3D_2$	21.95 ± 0.44	0.05	
$^3P_2$	17.16 ± 0.17	-0.55	0.58 ± 0.00
ϵ_2	-2.19 ± 0.11	0.10	
$^3F_2$	0.44 ± 0.17	0.06	
$^1F_3$	-5.74 ± 0.20	0.03	
$^3F_3$	-1.76 ± 0.23	-0.03	0.79 ± 0.00
$^3D_3$	2.98 ± 0.35	-0.40	
ϵ_3	7.69 ± 0.15	0.11	
$^3G_3$	-5.08 ± 0.35	-0.05	
$^1G_4$	1.46 ± 0.08	-0.03	
$^3G_4$	7.04 ± 0.28	0.08	
$^3F_4$	2.74 ± 0.09	0.00	
ϵ_4	-1.45 ± 0.06	-0.01	
		400.00 MeV	
$^1S_0$	-15.49 ± 0.41	-0.50	1.01 ± 0.00
$^3P_0$	-19.40 ± 0.47	0.61	0.58 ± 0.00
$^1P_1$	-32.48 ± 0.76	0.67	
$^3P_1$	-34.42 ± 0.28	0.54	3.54 ± 0.00
$^3S_1$	-3.01 ± 0.72	0.83	
ϵ_1	4.97 ± 0.42	-0.17	
$^3D_1$	-25.18 ± 0.50	-0.31	
$^1D_2$	11.90 ± 0.10	-0.50	7.27 ± 0.35
$^3D_2$	22.45 ± 0.36	0.11	

TABLE II. (*Continued*).

State	δ or ϵ (deg)	δ_{pp}-δ_{np} (deg)	ρ
		400.00 MeV	
$^3P_2$	18.20±0.20	−0.57	0.29±3.03
ϵ_2	−2.00±0.13	0.11	
$^3F_2$	0.04±0.16	0.05	0.82±0.00
$^1F_3$	−4.70±0.22	0.06	
$^3F_3$	−2.91±0.23	−0.02	3.42±0.00
$^3D_3$	4.65±0.32	−0.45	
ϵ_3	8.23±0.17	0.11	
$^3G_3$	−5.83±0.39	−0.05	
$^1G_4$	2.21±0.07	−0.05	1.80±0.00
$^3G_4$	7.96±0.27	0.06	2.03±0.00
$^3F_4$	3.42±0.07	0.00	
ϵ_4	−1.64±0.07	0.01	
$^1H_5$	−2.27±0.14	−0.04	
$^3H_5$	−1.30±0.12	−0.03	1.25±0.00
		450.00 MeV	
$^1S_0$	−19.88±0.50	−0.37	1.36±0.00
$^3P_0$	−24.91±0.46	0.66	2.34±0.00
$^1P_1$	−34.38±0.79	0.72	
$^3P_1$	−37.04±0.35	0.55	4.66±1.65
$^3S_1$	−6.97±0.74	0.84	
ϵ_1	4.87±0.46	−0.18	
$^3D_1$	−27.43±0.53	−0.35	
$^1D_2$	13.32±0.13	−0.53	10.75±0.31
$^3D_2$	20.76±0.45	0.16	
$^3P_2$	18.17±0.23	−0.57	−0.07±2.83
ϵ_2	−1.74±0.18	0.11	
$^3F_2$	−0.53±0.20	0.04	1.18±0.00
$^1F_3$	−4.97±0.37	0.07	
$^3F_3$	−2.79±0.16	−0.02	5.10±0.00
$^3D_3$	4.59±0.32	−0.47	
ϵ_3	8.25±0.21	0.11	
$^3G_3$	−5.14±0.42	−0.04	
$^1G_4$	2.57±0.08	−0.06	2.49±0.00
$^3G_4$	8.64±0.42	0.05	2.72±0.00
$^3F_4$	3.79±0.09	−0.01	
ϵ_4	−1.48±0.09	0.01	
$^1H_5$	−2.16±0.16	−0.04	
$^3H_5$	−1.13±0.20	−0.03	1.76±0.00
		500.00 MeV	
$^1S_0$	−22.87±0.47	−0.26	1.73±0.00
$^3P_0$	−26.64±0.42	0.70	0.11±7.44
$^1P_1$	−33.47±0.85	0.77	
$^3P_1$	−40.70±0.27	0.55	9.05±1.33
$^3S_1$	−11.46±0.93	0.84	
ϵ_1	7.22±0.61	−0.18	
$^3D_1$	−28.08±0.55	−0.38	
$^1D_2$	13.74±0.09	−0.56	15.74±0.18
$^3D_2$	18.04±0.48	0.21	
$^3P_2$	18.93±0.14	−0.58	2.38±1.40
ϵ_2	−1.18±0.11	0.11	
$^3F_2$	−1.03±0.13	0.04	1.64±0.00
$^1F_3$	−6.59±0.22	0.08	
$^3F_3$	−1.78±0.20	−0.01	5.36±0.50
$^3D_3$	3.60±0.27	−0.49	
ϵ_3	9.21±0.27	0.11	
$^3G_3$	−7.42±0.38	−0.04	

TABLE II. (*Continued*).

State	δ or ϵ (deg)	δ_{pp}-δ_{np} (deg)	ρ
		500.00 MeV	
$^1G_4$	2.67 ± 0.06	-0.06	3.27 ± 0.00
$^3G_4$	9.60 ± 0.37	0.04	3.42 ± 0.00
$^3F_4$	4.23 ± 0.05	-0.01	0.75 ± 0.00
ϵ_4	-1.74 ± 0.06	0.02	
$^1H_5$	-3.04 ± 0.15	-0.05	
$^3H_5$	-1.45 ± 0.12	-0.02	2.34 ± 0.00
$^3G_5$	-1.67 ± 0.22	-0.06	
		550.00 MeV	
$^1S_0$	-28.08 ± 0.43	-0.17	2.15 ± 0.00
$^3P_0$	-30.96 ± 0.45	0.73	7.37 ± 1.09
$^1P_1$	-28.89 ± 2.03	0.81	
$^3P_1$	-43.60 ± 0.27	0.56	3.53 ± 0.99
$^3S_1$	-15.76 ± 2.08	0.83	
ϵ_1	9.14 ± 1.52	-0.18	
$^3D_1$	-29.65 ± 1.23	-0.40	
$^1D_2$	12.82 ± 0.13	-0.58	18.49 ± 0.17
$^3D_2$	17.22 ± 1.02	0.26	
$^3P_2$	18.64 ± 0.18	-0.57	9.29 ± 0.47
ϵ_2	0.02 ± 0.17	0.10	
$^3F_2$	-1.63 ± 0.17	0.04	2.21 ± 0.00
$^1F_3$	-7.46 ± 0.70	0.09	
$^3F_3$	-0.67 ± 0.18	-0.01	9.57 ± 0.30
$^3D_3$	4.20 ± 0.68	-0.51	
ϵ_3	9.43 ± 0.44	0.12	
$^3G_3$	-6.72 ± 1.19	-0.04	
$^1G_4$	3.43 ± 0.07	-0.07	4.16 ± 0.00
$^3G_4$	11.94 ± 0.65	0.03	4.16 ± 0.00
$^3F_4$	4.54 ± 0.07	-0.02	1.41 ± 0.00
ϵ_4	-1.57 ± 0.08	0.02	
$^1H_5$	-2.57 ± 0.40	-0.05	
$^3H_5$	-0.90 ± 0.12	-0.02	2.98 ± 0.00
$^3G_5$	-0.75 ± 0.49	-0.06	
		600.00 MeV	
$^1S_0$	-30.87 ± 0.38	-0.09	2.63 ± 0.00
$^3P_0$	-33.42 ± 0.44	0.74	11.14 ± 1.09
$^1P_1$	-28.71 ± 1.89	0.84	
$^3P_1$	-46.03 ± 0.26	0.56	3.70 ± 1.00
$^3S_1$	-20.58 ± 1.76	0.82	
ϵ_1	8.20 ± 0.97	-0.17	
$^3D_1$	-32.08 ± 1.19	-0.43	
$^1D_2$	10.55 ± 0.16	-0.59	21.40 ± 0.15
$^3D_2$	15.03 ± 0.91	0.32	
$^3P_2$	18.91 ± 0.15	-0.57	14.31 ± 0.35
ϵ_2	0.96 ± 0.14	0.10	
$^3F_2$	-1.92 ± 0.15	0.03	2.89 ± 0.00
$^1F_3$	-7.54 ± 0.70	0.10	
$^3F_3$	-0.14 ± 0.15	-0.01	13.54 ± 0.24
$^3D_3$	3.03 ± 0.60	-0.52	
ϵ_3	9.91 ± 0.38	0.12	
$^3G_3$	-5.81 ± 0.72	-0.03	
$^1G_4$	3.62 ± 0.08	-0.08	5.19 ± 0.00
$^3G_4$	11.72 ± 0.52	0.02	4.93 ± 0.00
$^3F_4$	4.89 ± 0.06	-0.02	2.40 ± 0.00
ϵ_4	-1.45 ± 0.06	0.03	
$^3H_4$	0.41 ± 0.07	0.03	
$^1H_5$	-3.21 ± 0.36	-0.05	
$^3H_5$	-0.82 ± 0.09	-0.02	3.73 ± 0.00
$^3G_5$	-0.22 ± 0.34	-0.07	

TABLE II. (*Continued*).

State	δ or ϵ (deg)	δ_{pp}-δ_{np} (deg)	ρ
		650.00 MeV	
$^1S_0$	-33.53 ± 0.53	-0.03	3.17 ± 0.00
$^3P_0$	-36.87 ± 0.67	0.76	14.38 ± 1.29
$^1P_1$	-30.04 ± 1.56	0.87	
$^3P_1$	-47.15 ± 0.35	0.56	2.65 ± 1.01
$^3S_1$	-23.97 ± 0.98	0.80	
ϵ_1	9.39 ± 0.76	-0.17	
$^3D_1$	-31.28 ± 1.13	-0.44	
$^1D_2$	8.17 ± 0.25	-0.60	22.30 ± 0.17
$^3D_2$	13.09 ± 0.64	0.39	
$^3P_2$	18.44 ± 0.24	-0.56	18.23 ± 0.35
ϵ_2	1.46 ± 0.19	0.10	
$^3F_2$	-1.90 ± 0.22	0.03	3.58 ± 0.00
$^1F_3$	-7.60 ± 0.48	0.11	
$^3F_3$	0.28 ± 0.23	0.00	18.51 ± 0.24
$^3D_3$	3.16 ± 0.53	-0.53	
ϵ_3	9.94 ± 0.27	0.12	
$^3G_3$	-6.18 ± 0.54	-0.03	0.58 ± 0.00
$^1G_4$	4.09 ± 0.12	-0.08	6.35 ± 0.00
$^3G_4$	12.59 ± 0.34	0.02	5.75 ± 0.00
$^3F_4$	5.26 ± 0.12	-0.02	3.73 ± 0.00
ϵ_4	-1.41 ± 0.10	0.03	
$^3H_4$	0.73 ± 0.11	0.03	
$^1H_5$	-3.60 ± 0.28	-0.05	
$^3H_5$	-0.65 ± 0.12	-0.01	4.58 ± 0.00
$^3G_5$	0.03 ± 0.29	-0.07	
$^3H_6$	1.17 ± 0.06	0.02	-2.52 ± 0.00
		700.00 MeV	
$^1S_0$	-36.46 ± 0.62	0.02	3.77 ± 0.00
$^3P_0$	-42.48 ± 0.75	0.77	13.87 ± 1.38
$^1P_1$	-31.20 ± 1.99	0.90	
$^3P_1$	-49.11 ± 0.43	0.56	2.50 ± 1.02
$^3S_1$	-29.50 ± 1.32	0.78	
ϵ_1	9.24 ± 1.06	-0.17	
$^3D_1$	-32.46 ± 1.65	-0.46	
$^1D_2$	5.18 ± 0.38	-0.61	22.59 ± 0.34
$^3D_2$	11.04 ± 0.83	0.46	
$^3P_2$	16.31 ± 0.32	-0.55	21.62 ± 0.36
ϵ_2	1.23 ± 0.25	0.10	
$^3F_2$	-3.76 ± 0.30	0.03	4.12 ± 0.00
$^1F_3$	-7.44 ± 0.89	0.11	
$^3F_3$	-1.51 ± 0.31	0.00	22.34 ± 0.25
$^3D_3$	3.07 ± 0.61	-0.54	
ϵ_3	9.35 ± 0.32	0.12	
$^3G_3$	-7.79 ± 0.73	-0.03	0.67 ± 0.00
$^1G_4$	4.19 ± 0.15	-0.09	7.03 ± 0.55
$^3G_4$	11.95 ± 0.47	0.01	6.62 ± 0.00
$^3F_4$	5.40 ± 0.16	-0.03	5.29 ± 0.00
ϵ_4	-1.57 ± 0.12	0.03	
$^3H_4$	0.16 ± 0.14	0.02	
$^1H_5$	-4.80 ± 0.51	-0.05	
$^3H_5$	-0.93 ± 0.14	-0.01	5.53 ± 0.00
$^3G_5$	-1.07 ± 0.36	-0.07	
$^3H_6$	1.28 ± 0.07	0.02	-2.90 ± 0.00
		750.00 MeV	
$^1S_0$	-40.41 ± 0.68	0.06	4.40 ± 0.00
$^3P_0$	-44.60 ± 0.80	0.77	14.45 ± 1.43

TABLE II. (*Continued*).

State	δ or ϵ (deg)	δ_{pp}-δ_{np} (deg)	ρ
		750.00 MeV	
$^1P_1$	-26.91 ± 2.40	0.91	
$^3P_1$	-50.83 ± 0.40	0.57	2.19 ± 1.02
$^3S_1$	-30.32 ± 1.33	0.76	
ϵ_1	9.32 ± 2.04	-0.16	
$^3D_1$	-31.96 ± 1.90	-0.46	
$^1D_2$	3.40 ± 0.38	-0.62	22.78 ± 0.40
$^3D_2$	10.12 ± 1.80	0.52	
$^3P_2$	15.53 ± 0.29	-0.53	25.02 ± 0.36
ϵ_2	1.71 ± 0.26	0.09	
$^3F_2$	-3.36 ± 0.30	0.04	4.45 ± 0.00
$^1F_3$	-8.57 ± 0.96	0.12	
$^3F_3$	-3.40 ± 0.34	0.00	25.65 ± 0.26
$^3D_3$	3.84 ± 0.83	-0.55	
ϵ_3	10.80 ± 0.55	0.12	
$^3G_3$	-6.21 ± 0.71	-0.02	0.77 ± 0.00
$^1G_4$	4.54 ± 0.16	-0.10	8.49 ± 0.53
$^3G_4$	11.94 ± 1.29	0.01	7.53 ± 0.00
$^3F_4$	6.22 ± 0.13	-0.03	6.40 ± 0.59
ϵ_4	-1.29 ± 0.13	0.04	
$^3H_4$	0.63 ± 0.16	0.02	
$^1H_5$	-5.15 ± 0.60	-0.05	
$^3H_5$	-0.34 ± 0.16	0.00	6.56 ± 0.00
$^3G_5$	0.01 ± 0.34	-0.08	
ϵ_5	3.56 ± 0.39	0.04	
$^3I_5$	-3.05 ± 0.43	-0.04	
$^3I_6$	7.30 ± 0.39	0.08	
$^3H_6$	1.58 ± 0.06	0.02	-3.30 ± 0.00
		800.00 MeV	
$^1S_0$	-43.58 ± 0.45	0.10	5.06 ± 0.00
$^3P_0$	-47.03 ± 0.63	0.78	18.29 ± 1.38
$^1P_1$	-40.76 ± 3.11	0.94	
$^3P_1$	-52.06 ± 0.26	0.57	3.00 ± 1.02
$^3S_1$	-30.08 ± 1.81	0.75	0.59 ± 0.00
ϵ_1	11.44 ± 1.64	-0.16	
$^3D_1$	-26.14 ± 1.58	-0.47	
$^1D_2$	2.39 ± 0.30	-0.63	22.82 ± 0.32
$^3D_2$	7.42 ± 1.53	0.59	
$^3P_2$	12.94 ± 0.18	-0.51	25.37 ± 0.25
ϵ_2	1.68 ± 0.19	0.09	
$^3F_2$	-5.41 ± 0.20	0.04	4.61 ± 0.00
$^1F_3$	-9.54 ± 0.97	0.13	
$^3F_3$	-6.47 ± 0.28	0.00	25.93 ± 0.26
$^3D_3$	5.81 ± 0.58	-0.56	-0.62 ± 0.00
ϵ_3	12.49 ± 0.54	0.12	
$^3G_3$	-5.32 ± 0.64	-0.02	0.87 ± 0.00
$^1G_4$	4.68 ± 0.12	-0.10	8.69 ± 0.43
$^3G_4$	11.90 ± 1.40	0.01	8.48 ± 0.00
$^3F_4$	6.26 ± 0.08	-0.04	8.47 ± 0.40
ϵ_4	-1.50 ± 0.10	0.04	
$^3H_4$	0.84 ± 0.13	0.02	
$^1H_5$	-2.91 ± 0.71	-0.06	
$^3H_5$	-0.19 ± 0.12	0.00	7.87 ± 0.35
$^3G_5$	0.01 ± 0.22	-0.08	
ϵ_5	3.68 ± 0.44	0.04	
$^3I_5$	-4.24 ± 0.24	-0.04	
$^3I_6$	7.12 ± 0.59	0.07	
$^3H_6$	1.74 ± 0.03	0.02	-3.72 ± 0.00

TABLE II. (*Continued*).

State	δ or ϵ (deg)	δ_{pp}-δ_{np} (deg)	ρ
		850.00 MeV	
$^1S_0$	-43.57 ± 1.39	0.14	5.73 ± 0.00
$^3P_0$	-46.46 ± 1.54	0.78	19.34 ± 1.71
$^1P_1$	-27.81 ± 4.85	0.95	
$^3P_1$	-53.11 ± 0.55	0.57	2.84 ± 1.02
$^3S_1$	-34.71 ± 9.97	0.73	0.66 ± 0.00
ϵ_1	6.90 ± 5.13	-0.16	
$^3D_1$	-34.80 ± 11.02	-0.47	
$^1D_2$	1.91 ± 0.57	-0.63	22.59 ± 0.67
$^3D_2$	1.92 ± 2.81	0.66	
$^3P_2$	10.38 ± 0.76	-0.49	28.60 ± 0.59
ϵ_2	0.76 ± 0.35	0.08	
$^3F_2$	-5.47 ± 0.33	0.04	4.68 ± 0.00
$^1F_3$	-8.79 ± 1.00	0.13	
$^3F_3$	-10.03 ± 0.57	0.01	26.74 ± 0.47
$^3D_3$	6.01 ± 2.13	-0.56	-0.68 ± 0.00
ϵ_3	8.45 ± 2.23	0.12	
$^3G_3$	-8.05 ± 1.32	-0.02	0.97 ± 0.00
$^1G_4$	5.22 ± 0.27	-0.11	11.23 ± 0.62
$^3G_4$	14.91 ± 0.83	0.01	9.45 ± 0.00
$^3F_4$	6.18 ± 0.23	-0.04	9.41 ± 0.61
ϵ_4	-1.45 ± 0.16	0.04	
$^3H_4$	0.22 ± 0.20	0.02	
$^1H_5$	-5.98 ± 0.49	-0.05	
$^3H_5$	-0.05 ± 0.39	0.00	7.32 ± 0.68
$^3G_5$	-1.68 ± 1.27	-0.09	
ϵ_5	3.18 ± 1.07	0.04	
$^3I_5$	-4.51 ± 0.99	-0.04	
$^3I_6$	5.60 ± 0.67	0.07	
$^3H_6$	1.69 ± 0.10	0.02	-4.15 ± 0.00
		900.00 MeV	
$^1S_0$	-45.71 ± 1.21	0.16	6.40 ± 0.00
$^3P_0$	-49.44 ± 1.32	0.78	25.57 ± 1.80
$^1P_1$	-25.29 ± 3.84	0.97	
$^3P_1$	-53.54 ± 0.76	0.56	3.10 ± 1.03
$^3S_1$	-42.20 ± 3.79	0.71	0.72 ± 0.00
ϵ_1	6.33 ± 4.97	-0.15	
$^3D_1$	-34.96 ± 3.95	-0.47	
$^1D_2$	0.04 ± 0.57	-0.63	23.43 ± 0.60
$^3D_2$	0.15 ± 3.32	0.73	
$^3P_2$	7.08 ± 0.65	-0.47	28.74 ± 0.71
ϵ_2	0.94 ± 0.34	0.08	
$^3F_2$	-5.96 ± 0.37	0.05	4.70 ± 0.00
$^1F_3$	-7.19 ± 0.71	0.14	
$^3F_3$	-13.96 ± 0.60	0.01	25.38 ± 0.59
$^3D_3$	4.59 ± 1.37	-0.57	-0.75 ± 0.00
ϵ_3	10.56 ± 1.41	0.12	
$^3G_3$	-8.29 ± 1.05	-0.02	1.07 ± 0.00
$^1G_4$	5.10 ± 0.31	-0.11	12.39 ± 0.56
$^3G_4$	12.13 ± 0.81	0.01	10.42 ± 0.00
$^3F_4$	6.66 ± 0.30	-0.05	9.80 ± 0.71
ϵ_4	-1.71 ± 0.17	0.04	
$^3H_4$	0.36 ± 0.28	0.02	
$^1H_5$	-7.02 ± 0.44	-0.05	
$^3H_5$	0.10 ± 0.29	0.00	10.07 ± 0.65
$^3G_5$	-0.16 ± 0.96	-0.09	
ϵ_5	1.26 ± 0.65	0.04	
$^3I_5$	-2.51 ± 0.90	-0.04	

TABLE II. (*Continued*).

State	δ or ϵ (deg)	δ_{pp}-δ_{np} (deg)	ρ
		900.00 MeV	
$^1I_6$	2.29±0.16	−0.03	6.62±0.00
$^3I_6$	9.10±0.74	0.07	
$^3H_6$	2.17±0.13	0.01	−4.60±0.00
ϵ_6	−1.62±0.13	0.00	
		950.00 MeV	
$^1S_0$	−47.51±1.30	0.19	7.07±0.00
$^3P_0$	−49.24±1.36	0.78	23.74±1.94
$^3P_1$	−54.99±0.69	0.56	3.20±1.03
$^1D_2$	−0.03±0.53	−0.62	25.10±0.75
$^3P_2$	2.10±0.68	−0.45	29.86±0.84
ϵ_2	1.01±0.52	0.07	
$^3F_2$	−7.20±0.63	0.05	4.70±0.00
$^3F_3$	−12.23±0.62	0.01	24.03±0.59
$^1G_4$	3.73±0.34	−0.12	12.26±0.65
$^3G_4$	5.90±0.28	−0.05	10.56±0.75
ϵ_4	−1.91±0.24	0.04	
$^3H_4$	0.44±0.33	0.02	
$^3H_5$	0.93±0.31	0.00	12.70±0.62
$^1I_6$	1.71±0.14	−0.03	7.31±0.00
$^3H_6$	1.82±0.12	0.01	−5.05±0.00
ϵ_6	−1.29±0.13	0.00	
		999.00 MeV	
$^1S_0$	−49.03±1.23	0.20	7.71±0.00
$^3P_0$	−56.25±1.18	0.78	27.85±1.98
$^3P_1$	−56.47±0.47	0.56	3.27±1.03
$^1D_2$	−1.89±0.50	−0.61	25.19±0.63
$^3P_2$	1.80±0.57	−0.43	33.35±0.56
ϵ_2	1.88±0.37	0.07	
$^3F_2$	−7.56±0.41	0.06	4.70±0.00
$^3F_3$	−13.29±0.40	0.01	22.26±0.43
$^1G_4$	4.24±0.27	−0.12	13.52±0.59
$^3F_4$	5.97±0.17	−0.06	10.64±0.58
ϵ_4	−1.62±0.15	0.05	
$^3H_4$	−0.42±0.20	0.02	
$^3H_5$	0.69±0.19	0.01	13.86±0.42
$^1I_6$	2.44±0.11	−0.03	7.98±0.00
$^3H_6$	2.14±0.06	0.01	−5.50±0.00
ϵ_6	−1.41±0.11	0.00	
		1050.00 MeV	
$^1S_0$	−48.01±1.46	0.22	8.37±0.00
$^3P_0$	−60.22±1.36	0.78	33.73±2.07
$^3P_1$	−57.85±0.54	0.56	3.50±1.03
$^1D_2$	−2.50±0.54	−0.60	24.46±0.66
$^3P_2$	0.17±0.66	−0.40	33.29±0.55
ϵ_2	2.04±0.44	0.06	
$^3F_2$	−8.77±0.49	0.06	4.69±0.00
$^3F_3$	−14.68±0.68	0.01	22.35±0.38
$^1G_4$	5.55±0.37	−0.12	15.27±0.58
$^3F_4$	6.57±0.21	−0.06	10.27±0.64
ϵ_4	−2.35±0.18	0.05	
$^3H_4$	−0.03±0.22	0.02	
$^3H_5$	−0.10±0.32	0.01	14.78±0.39
$^1I_6$	2.60±0.15	−0.03	8.67±0.00
$^3H_6$	2.24±0.07	0.01	−5.96±0.00
ϵ_6	−1.12±0.14	0.00	

TABLE II. (*Continued*).

State	δ or ϵ (deg)	δ_{pp}-δ_{np} (deg)	ρ
		1100.00 MeV	
$^1S_0$	-49.82 ± 1.92	0.24	9.00 ± 0.00
$^3P_0$	-60.95 ± 1.78	0.77	37.86 ± 2.24
$^3P_1$	-59.42 ± 0.70	0.56	3.59 ± 1.04
$^1D_2$	-3.57 ± 0.60	-0.59	24.06 ± 0.55
$^3P_2$	-4.00 ± 0.89	-0.38	34.26 ± 0.72
ϵ_2	0.53 ± 0.58	0.05	
$^3F_2$	-10.38 ± 0.67	0.07	4.68 ± 0.00
$^3F_3$	-16.75 ± 0.73	0.02	22.25 ± 0.47
$^1G_4$	6.30 ± 0.40	-0.13	16.59 ± 0.54
$^3F_4$	5.18 ± 0.40	-0.07	10.24 ± 0.81
ϵ_4	-2.97 ± 0.25	0.05	
$^3H_4$	-0.78 ± 0.31	0.02	
$^3H_5$	-1.43 ± 0.45	0.01	15.38 ± 0.48
$^1I_6$	2.08 ± 0.20	-0.04	9.33 ± 0.00
$^3H_6$	1.50 ± 0.20	0.01	-6.41 ± 0.00
ϵ_6	-0.46 ± 0.22	0.00	

other states, due to its higher energy and smaller coupling to NN.

VI. CONCLUSIONS; USE OF SAID

A recently improved and expanded NN elastic scattering data base has been used to extract partial waves to 1100 MeV. The global solution, SM86, and 22 single-energy solutions reveal tightly constrained $I=1$ waves below 800 MeV and loosely determined $I=0$ waves above 500 MeV. This is a consequence of the far greater abundance of pp scattering data over np data; an imbalance which has been exacerbated in recent years.

The solutions give clear indications of resonance behavior in the $^1D_2$, $^3F_3$, $^3P_2$-$^3F_2$, and $^3F_4$-$^3H_4$ partial waves. A new form of parametrization was used for the global solution SM86, which allows a mapping of the T matrix in the complex energy plane and the extraction of pole positions and residues which are associated with the observed structures.

Detailed examination of these and several other solutions can be accomplished through the scattering analysis interactive dial-in (SAID) system, which is accessible on VPI&SU computers. SAID includes the data base and solution files along with interactive FORTRAN77 programs used to display the multitude of quantities predicted from the solutions. (SAID also contains the VPI&SU πN and K^+N analyses results.) SAID is also packaged on VAX backup tapes which can be easily transported for use on DEC VAX computers at other sites. Over 100 sites around the world now use SAID.

The two-body elastic amplitudes can also be encoded, using SAID, in a binary-coded decimal (BCD) file, which is then used by a subroutine, NNAMP, to give very accurate

TABLE III. Pole parameters for $^1D_2$, $^3F_3$, $^3P_2$-$^3F_2$, and $^3F_4$-$^3H_4$ states. W_p is the pole position in MeV. G (modulus phase) is the function $(W_p-W)T_p$ evaluated at the pole; it is the residue of T_p at the pole. $G_r=\mathrm{Re}G$ and $G_i=\mathrm{Im}G$.

State	W_p (MeV)	$\lvert G \rvert$ (MeV)	$\arctan(G_i/G_r)$ (deg)
$^1D_2$	$2148-i63$	10	-15
$^3F_3$	$2183-i79$	14	-78
$^3P_2$	$2163-i75$	7.7	52
$^3F_2$	$2163-i75$	0.28	86
$^3F_4$	$2210-i78$	1.2	87
$^3H_4$	$2210-i78$	0.04	-41

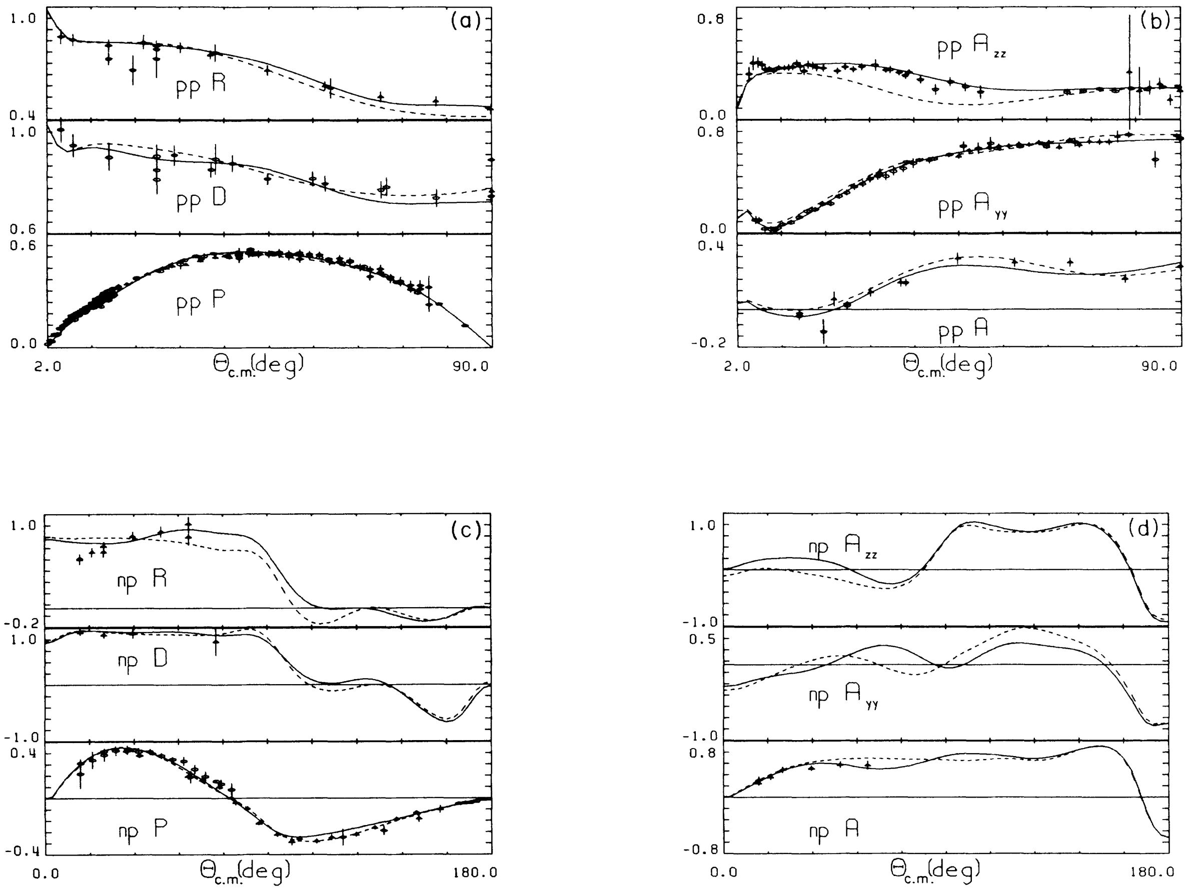

FIG. 4. Scattering observables at 800 MeV. Most of the data shown are recent LAMPF measurements.

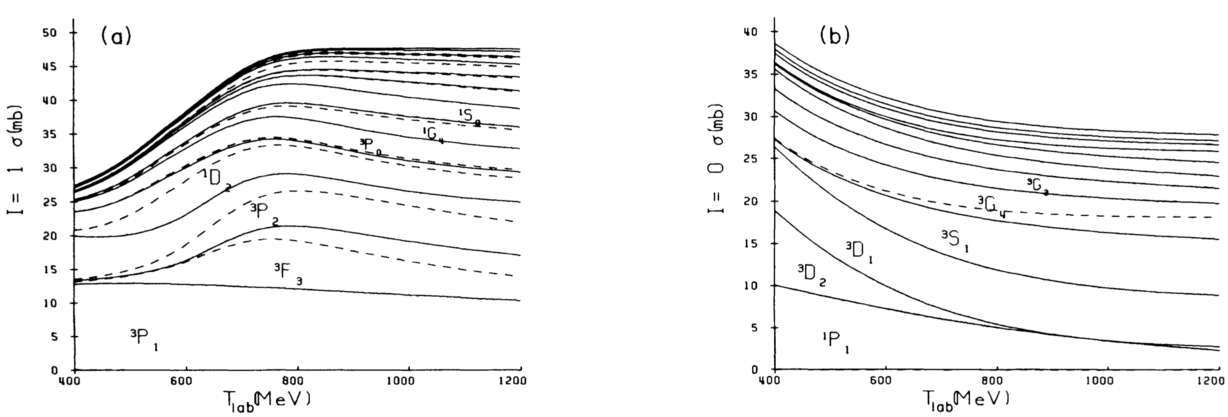

FIG. 5. Cumulative partial-wave cross sections for $I=1$ (a) and for $I=0$ (b). Solid lines represent total cross sections and dashed lines represent inelastic cross sections (excluding spin-flip elastic).

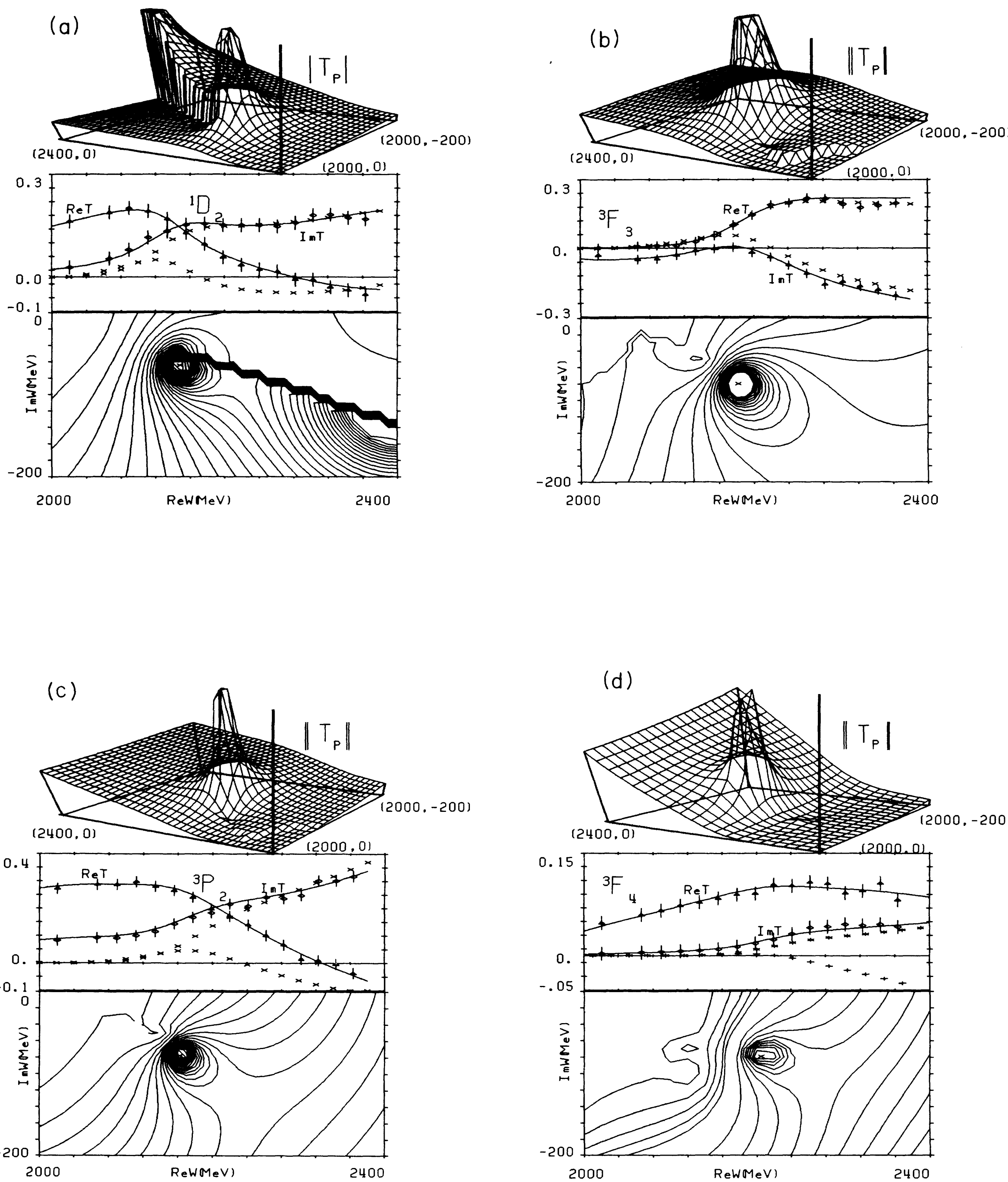

FIG. 6. Complex-energy-plane plots for states exhibiting "resonancelike" structure ($^2D_2$, $^3F_3$, $^3P_2$, and $^3F_4$). Bottom plot is a contour mapping of $|T_p|$ for $2000 < \mathrm{Re}W < 2400$ MeV, and $-200 < \mathrm{Im}W < 0$ MeV. The center plot is the T matrix; $\times$'s are used to plot T_p. The top plot is a three-dimensional representation of $|T_p|$; the forward edge is the physical axis ($\mathrm{Im}\,W = 0$).

amplitude reconstructions below 1 GeV. This allows the solution to be used calculationally, e.g., in N-nuclear reactions. Both partial-wave and summed (helicity) amplitudes are obtained at each specified kinematic point (energy, angle). The interpolating array, NNAMP, and all supporting subroutines are available from VPI&SU and can be sent via Bitnet to any connected computer.

ACKNOWLEDGMENTS

This work was sponsored by United States Department of Energy Contract No. DE-AS05-76-ER04928. The authors are grateful to a large number of colleagues who have made suggestions regarding these analyses and the SAID program.

[1]R. A. Arndt, L. D. Roper, R. A. Bryan, R. C. Clark, B. J. VerWest, and P. Signell, Phys. Rev. D **28**, 97 (1983). The +, − subscripts on S in Eqs. (7) should be reversed.

[2]P. W. Lisowski, R. E. Shamu, G. F. Auchampaugh, N. S. P. King, M. S. Moore, G. L. Morgan, and T. S. Singleton, Phys. Rev. Lett. **49**, 255 (1982).

[3]R. A. Arndt, R. Hackman, and L. D. Roper, Phys. Rev. C **15**, 1002 (1977).

[4]R. A. Arndt, John Ford, and L. D. Roper, Phys. Rev. D **32**, 1085 (1985).